JOURNAL OF BACTERIOLOGY, Apr. 1997, p. 2401–2409 Vol. 179, No. 7
0021-9193/97/$04.00+0

Interactions of OxyR with the Promoter Region of the *oxyR* and *ahpC* Genes from *Mycobacterium leprae* and *Mycobacterium tuberculosis*

S. DHANDAYUTHAPANI,[1] M. MUDD,[2] AND V. DERETIC[2]*

Department of Microbiology, University of Texas Health Science Center at San Antonio, San Antonio, Texas 78284-7758,[1] and Department of Microbiology and Immunology, University of Michigan Medical School, Ann Arbor, Michigan 48109-0620[2]

Received 2 October 1996/Accepted 29 January 1997

In contrast to the intact *oxyR* gene (a homolog of the central regulator of peroxide stress response in enteric bacteria) in *Mycobacterium leprae*, this gene is inactive in all strains of *M. tuberculosis*. In both species, *oxyR* is divergently transcribed from *ahpC*, which encodes a homolog of alkyl hydroperoxide reductase. To initiate investigations of the regulation of oxidative stress in mycobacteria and consequences of the elimination of *oxyR* in *M. tuberculosis*, in this work we tested the hypothesis that mycobacterial OxyR acts as a DNA binding protein and analyzed its interactions with the *oxyR* and *ahpC* promoters. *M. leprae* OxyR was overproduced and purified, and its binding to the *oxyR-ahpC* intergenic region of *M. leprae* was demonstrated. By using a sequential series of overlapping DNA fragments, the minimal OxyR binding site was delimited to a 30-bp DNA segment which included a palindromic sequence conforming with the established rules for the LysR family of regulators. A consensus sequence for the mycobacterial OxyR recognition site (cTTATCggc-N_3-gccGATAAg) was deduced based on its conservation in different mycobacteria. A variance in two potentially critical nucleotides within this site was observed in *M. tuberculosis*, in keeping with its reduced affinity for OxyR. Transcription of plasmid-borne *M. leprae oxyR* and *ahpC* was investigated in *M. smegmatis* and *M. bovis* BCG by S1 nuclease protection and transcriptional fusion analyses. Two mRNA 5′ ends were detected in each direction: (i) P_1*oxyR* and P_2*oxyR* and (ii) P_1*ahpC* and P_2*ahpC*. The binding site for OxyR overlapped P_1*oxyR*, reminiscent of the autoregulatory loops controlling expression of *oxyR* in enteric bacteria and characteristic of the LysR superfamily in general. This site was also centered 65 bp upstream of P_1*ahpC*, matching the usual position of LysR-type recognition sequences in relationship to positively controlled promoters. Superimposed on these features was the less orthodox presence of multiple transcripts and their unique arrangement, including a region of complementarity at the 5′ ends of the P_2*ahpC* and P_2*oxyR* mRNAs, suggesting the existence of complex regulatory relationships controlling *oxyR* and *ahpC* expression in mycobacteria.

The adaptation mechanisms that enable the potent human pathogens *Mycobacterium tuberculosis* and *M. leprae* to thrive in the intracellular environment of susceptible mononuclear phagocytic cells are not completely understood despite several recent advances (8, 14, 29, 45). Of potential significance for the successful parasitism of host macrophages is the response of mycobacteria to oxidative stress since reactive oxygen and nitrogen species are likely to be encountered during interactions with phagocytic cells (22). In a recent series of studies (10, 11, 13, 16, 38, 50) aimed at analyzing oxidative stress response in *M. tuberculosis*, we and others have characterized the gene *oxyR*, encoding a homolog of the central regulator of peroxide stress response in enteric bacteria (7, 46). In *Escherichia coli* and *Salmonella typhimurium*, *oxyR* positively regulates at least nine genes (7, 46), including those encoding catalase-peroxidase (*katG*), alkyl hydroperoxide reductase (*ahpC*), glutathione oxidoreductase (*gorA*), a protein implicated in protection of DNA from oxidants (*dps*), and a small untranslated regulatory RNA (*oxyS*). Surprisingly, the *oxyR* gene in *M. tuberculosis* displays multiple lesions (11, 38). The mutations in *oxyR*, which render this gene inactive, have been observed in all strains of *M. tuberculosis* tested (11) and, with minor variations (42), in all members of the *M. tuberculosis* complex: *M. africanum*, *M. bovis*, and *M. microti* (11). In contrast, intact *oxyR* genes have been characterized in *M. leprae* (11, 38) and *M. avium* (38). The *oxyR* gene is likely to be complete in *M. marinum* and *M. xenopi* and possibly also in *M. gastri*, *M. kansasii*, and *M. scrofulaceum* (11). In the majority of mycobacterial species tested, *oxyR* is tightly linked to and divergently transcribed from *ahpC* (10, 11, 37, 38, 47, 48), a gene encoding a homolog of the catalytic subunit of alkyl hydroperoxide reductase (4, 7, 21). Two notable exceptions to these generalizations are *M. smegmatis* and *M. aurum*, in which *oxyR* could not be positively identified by PCR or hybridization (13). Although *M. smegmatis* has an *ahpC* equivalent, no potential OxyR-encoding sequences could be detected within the 900-bp region characterized immediately upstream of the *ahpC* gene (13); the existence and location of *oxyR* or its putative functional equivalent in this species remain to be determined.

Possibly related to the lack of *oxyR* function in *M. tuberculosis* (10, 11, 50), this mycobacterium exhibits exceptionally high susceptibility to the front-line antituberculosis drug isonicotinic acid hydrazide (isoniazid; INH). Based on their intrinsic sensitivities to INH, mycobacteria fall into two general categories (49, 52): (i) most species are susceptible only to INH concentrations in excess of 1 μg/ml, and (ii) a small number of organisms, encompassing members of the *M. tuberculosis* complex and a fast-growing saprophytic species, *M. aurum* (13, 27), display high sensitivities to this compound. *M. tuberculosis* is

* Corresponding author. Mailing address: Department of Microbiology and Immunology, 5641 Medical Science Building II, University of Michigan Medical School, Ann Arbor, MI 48109-0620. Phone: (313) 763-1580. Fax: (313) 647-6243. E-mail: Deretic@umich.edu.

susceptible to exceptionally low levels of INH, in the range of 0.02 to 0.06 μg/ml (49). In a recent study (13), an inverse correlation has been noted between the intrinsic sensitivity to INH in mycobacterial species on one side and AhpC levels and overall ability to mount a peroxide stress response on the other. Furthermore, recent insertional inactivation of *ahpC* on the chromosome of *M. smegmatis* has demonstrated that AhpC levels determine the baseline sensitivity of mycobacteria to INH (50), further supporting the notion that lesions in *oxyR*, a putative regulator of *ahpC* expression, may contribute to the exquisite sensitivity of *M. tuberculosis* to INH (10). As a result of a long history of studies antecedent to the more recent research directions described above, another member of the putative peroxide stress response in *M. tuberculosis* has been shown to play a central role in the processes associated with INH resistance. These important investigations aimed at understanding the emergence of INH-resistant *M. tuberculosis* strains in clinical practice (19, 30, 32, 51) have established that *katG*, encoding *M. tuberculosis* catalase-peroxidase, plays a major role in the emergence of INH resistance. Interestingly, expression of the *katG* gene appears not to be adversely affected by the loss of OxyR function in wild-type *M. tuberculosis* strains which display substantial catalase-peroxidase activity.

The proposals that mycobacterial OxyR plays a regulatory role have been based on its sequence similarities to OxyR from enteric bacteria and other members of the LysR family of transcriptional regulators (18). However, this hypothesis has not been formally addressed. The majority of proteins from the LysR superfamily positively control expression of their cognate target genes while frequently playing a negative autoregulatory role. Among the hallmarks of these relationships are the arrangement of binding sites within the respective promoter regions and the organization of transcriptional units (36). By analogy with other LysR family members, it is possible that mycobacterial OxyR functions as a DNA binding protein and transcriptional regulator. As a step towards a formal demonstration of these putative relationships, we report here the mapping of the mRNA 5′ ends for the *M. leprae oxyR* and *ahpC* genes expressed in fast- and slow-growing mycobacterial hosts, the overproduction and purification of *M. leprae* OxyR, and the interactions of OxyR with the promoter region of *oxyR* and *ahpC* in *M. leprae* and *M. tuberculosis*.

MATERIALS AND METHODS

Bacterial strains and growth conditions. The mycobacterial strains used in this study were *M. smegmatis* mc^{2}155 (41) and *M. bovis* BCG ATCC 27291. *Escherichia coli* DH5α and BL21(DE3)pLysS were used for routine cloning or overexpression of *M. leprae* OxyR, respectively. Mycobacteria were grown in Middlebrook 7H9 medium or on 7H10 plates (Difco Laboratories) supplemented with 0.05% Tween 80 and ADC enrichments. When necessary, kanamycin or hygromycin was added to 10 or 50 μg/ml, respectively. All incubations were at 37°C.

RNA isolation, S1 nuclease protection assay, and primer extension analysis. Isolation of RNA from mycobacteria by sedimentation through a cushion of 5.7 M CsCl has been previously described (9, 13, 50). Primers OxyRML7 (5′-GCC TGCGACAACGTCGAC-3′; extending from −234 to −217 relative to the *ahpC* start codon; see Fig. 2A) and AhpML7 (5′-CCTTTGATAAGTCGCCGC-3′; extending from +76 to +59; see Fig. 2A) were used to generate uniformly labeled (using [α-^{32}P]dCTP, 800 Ci/mmol; DuPont NEN) single-stranded probes to map the 5′ ends of *M. leprae oxyR* and *ahpC* transcripts, respectively. The S1 nuclease protection assay was carried out as previously described (9, 13, 50). Plasmid pDML2, denatured by treatment with NaOH, was used as a template to generate single-stranded hybridization probes. Each hybridization reaction contained 50 μg of total RNA. The products of S1 nuclease digestion were analyzed on sequencing gels and compared with the sequencing ladder generated by using the primers OxyRML7 and AhpML7 to locate the 5′ end of mRNA. Since the probes were uniformly labeled to improve the sensitivity of the assay as previously described (9, 13, 50), the heterogeneity at the 5′ ends of S1 nuclease digestion products was more prominent due to the radioactive decay-related breakdown of single-stranded DNA chains (3). Primer extension analysis was carried out as previously described (1), by using OxyRML7 for *oxyR* mRNA and AhpM8 (5′TGTTGGCCAATTGATAGCAATGACATATCC3′) for *ahpC* mRNA and equal amounts of RNA as for S1 nuclease protection studies.

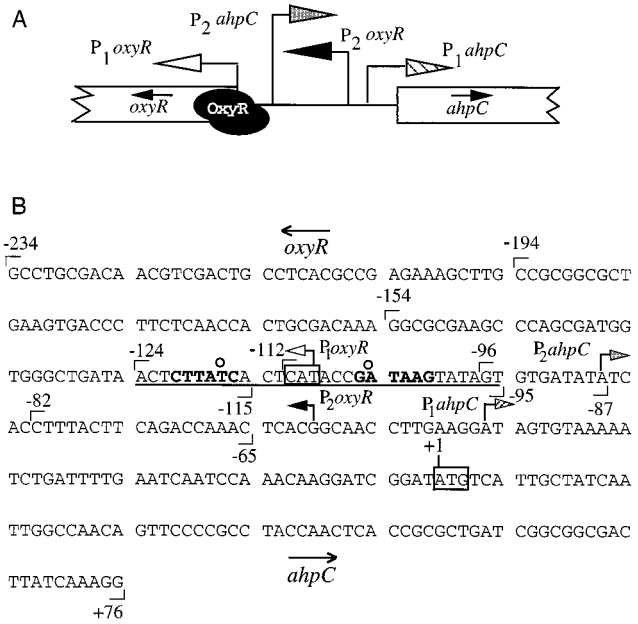

FIG. 1. *M. leprae* intergenic region, *oxyR* and *ahpC* mRNA start sites, and OxyR binding site. (A) Schematic representation of the *oxyR-ahpC* intergenic region. (B) Locations of the *oxyR* and *ahpC* mRNA start sites and summary of the PCR-based strategy for mapping of the OxyR binding site within the *M. leprae oxyR-ahpC* intergenic region. Bent arrows, mRNA start sites; open arrowheads, mRNA start site P_1*oxyR*; filled arrowheads, P_2*oxyR*; hatched arrowheads, P_1*ahpC*; stippled arrowheads, P_2*ahpC*; double oval, bound OxyR; boxed nucleotides, *oxyR* and *ahpC* start codons; bent lines and numbers, 5′ ends of the primers relative to the *ahpC* start codon. Primer direction is shown by placement above or below the sequence. These primers were used to generate by PCR a sequential series of overlapping DNA fragments for OxyR binding studies. Underlined nucleotides, deduced region containing the OxyR binding site. Bold residues, proposed OxyR recognition sequence. The T-N_{11}-A core (17, 36) is indicated by circles above the nucleotides.

Plasmid constructs and genetic methods. *oxyR* overexpression plasmid pDML1 was generated by modifying the ends of *M. leprae oxyR* by PCR with primers MLoxyRFW (5′ATACTTATCCATATGAGTGATAAG 3′ [the *Nde*I site is underlined]) and MLoxyRRV (5′TGGCATGGGCTCGAGGACGATCTC 3′ [the *Xho*I site is underlined]). The product was cloned into the vector pCRII (Invitrogen), excised as an *Nde*I-*Xho*I fragment, and inserted into the corresponding sites of the T7 expression vector pET16-6 (Novagen) to generate plasmid pDML1. The insert sequence and its in-frame fusion within the polylinker region of the T7 vector were verified by sequencing. Plasmid pDML2 was constructed as follows: a 2-kb PCR fragment containing the complete coding regions of *M. leprae oxyR* and *ahpC* was generated by using primers OxyR6ML (5′-GGTTTG CCGGTACCCGAACTGC-3′) and Ahp6ML (5′-GTGTCGACTCCCGGGTT GGCGATG-3′). The resulting PCR fragment was cloned into pCRII, and upon confirmation of the DNA sequence the insert was excised as an *Spe*I-*Xba*I fragment and subcloned into the *Xba*I site of the mycobacterial-*E. coli* shuttle vector pOLYG (15). To generate *ahpC-xylE* transcriptional fusion plasmids pDMLAX and pDMLAX/O, a 1.1-kb PCR fragment encompassing the *M. leprae oxyR-ahpC* intergenic region was produced by using previously described primers Ahp1P and OxyR1P (11). This fragment was subcloned into pCRII, excised as an *Eco*RI fragment, and cloned into *xylE* transcriptional fusion plasmid pHSX2 (9) to generate pDMLAX. To examine the effects of *oxyR*, this plasmid was modified by excising the 1.3-kb *Eco*RI fragment from plasmid pDML2, carrying the complete *oxyR* sequence from *M. leprae*, and inserting this fragment (blunt ended) into the *Hpa*I site of pDMLAX, resulting in pDMLAX/O. Plasmid pVDtb#3, a subclone of the genomic *M. tuberculosis* H37Rv *oxyR-ahpC* region, has been previously described (11, 13). Plasmids were introduced into *M. smegmatis* mc^{2}155 or *M. bovis* BCG Pasteur as previously described (20).

Generation of a series of overlapping PCR fragments for protein-DNA binding studies. The following oligonucleotide primers were used to generate a series of overlapping fragments spanning the *oxyR-ahpC* intergenic region of *M. leprae* (the 5′ and 3′ ends, respectively, relative to the *ahpC* start codon, as shown in Fig. 1, are indicated): OxyRML7 (5′-GCCTGCGACAACGTCGAC-3′; −234 and −217), OxyRML8 (5′-CTTTACTTCAGACCAAAC-3′; −82 and −65),

OxyRML9 (5′-GTGTGATATATCACCTTT-3′; −96 and −79), OxyRML10 (5′-CATACCGATAAGTATAGT-3′; −112 and −95), OxyRML11 (5′-GGCGCG AAGCCCAGCGAT-3′; −154 and −136), OxyRML12 (5′-CCGCGGCGCTGA AGTGAC-3′; −194 and −177), OxyRML13 (5′-GTTTGGTCTGAAGTAAAG -3′; −65 and −82), OxyRML14 (5′ACTCTTATCACTCATACC-3′; −124 and −117), OxyRML15 (5′-TATATCACACTATACTTA-3′; −87 and −104), OxyRML16 (5′-ACTATACTTATCGGTATG-3′; −95 and −112), OxyRML17 (5′-TGATAAGAGTTATCAGCC-3′; −115 and −132), and AhpML7 (5′-CCT TTGATAAGTCGCCGC-3′; +76 and +59). In the case of *oxyR-ahpC* from *M. tuberculosis*, the primers used were OxyRTB7 (5′-CGAAGCCCGGCCACGGC C-3′; −146 and −129) and Ahp4 (5′-GGTGAAGTAGTCGCCGGGT-3′; +104 and +87). DNA amplification was carried out by using standard PCR protocols with plasmid pDML2 or pVDtb#3 as the template.

Overproduction and purification of *M. leprae* OxyR. *M. leprae* OxyR was overproduced and purified as a hybrid protein with a His_{10} tag fused to its N terminus. An overnight culture (1 ml) of *E. coli* BL21(DE3)LysS harboring pDML1 was inoculated into 200 ml of fresh Luria broth and grown to an A_{600} of 0.4. Isopropyl-β-D-thiogalactopyranoside (IPTG) was added to 1 mM, incubation at 37°C was continued for another 2 h, and bacteria were harvested by centrifugation at 3,000 rpm. The cells were resuspended in a buffer (5 ml/g [wet weight]) containing 20 mM Tris-HCl (pH 7.6) and 500 mM NaCl and lysed by three passages through a French press. The lysate was clarified by centrifugation at 3,000 rpm for 15 min, and the resulting supernatant was centrifuged again at 10,000 rpm for 30 min. His_{10}-OxyR partitioned with the insoluble 10,000-rpm-centrifuged sediment. The OxyR-enriched pellet was resuspended in a solubilization buffer (5 ml/g [wet weight]) containing 8 M urea, 100 mM sodium phosphate, and 10 mM Tris-HCl (pH 8.0) by stirring for 2 h. The extract was centrifuged at 10,000 rpm for 15 min to remove the insoluble residue, and 2 ml of a 50% slurry of Ni-nitrilotriacetic acid (NTA) resin (Qiagen) was added to the supernatant. After being stirred for 3 h, the slurry was packed into a column. The column was washed with the same buffer used to solubilize His_{10}-OxyR. His_{10}-OxyR bound to the Ni-NTA resin was eluted with elution buffer (200 mM imidazole, 8 M urea, 100 mM sodium phosphate; 10 mM Tris-HCl [pH 7.6]). The eluted material was analyzed by sodium dodecyl sulfate-polyacrylamide gel electrophoresis (SDS-PAGE), and fractions enriched in OxyR were pooled and dialyzed against a series of buffers with stepwise decreases in the urea concentration (10 mM Tris-HCl [pH 7.6] plus urea at 6, 4, 2, and 1 M) for 1 h at each urea concentration. Finally, the protein solution was dialyzed against the storage buffer containing 10 mM Tris-HCl (pH 7.6), 100 mM KCl, 10 mM $MgCl_2$, 1 mM EDTA, and 50% glycerol. At this stage, some precipitate formed and was removed by centrifugation. The final preparation was aliquoted and stored at −20°C.

Mobility shift protein-DNA binding assay. DNA probes were end labeled with [γ-^{32}P]ATP (6,000 Ci/mmol; DuPont NEN) by using T4 polynucleotide kinase and purified by electrophoresis on 5% polyacrylamide gels followed by electroelution. The standard protein-DNA binding reaction mixture contained 20,000 cpm of probe DNA and 250 ng of purified His_{10}-OxyR in 10 μl of binding buffer [25 mM Tris-HCl (pH 8.0), 6 mM $MgCl_2$, 0.5 mM EDTA, 20 mM KCl, 0.5 mM dithiothreitol (DTT), 100 μg of poly(dI-dC) (Pharmacia-Biotech) per ml, 100 μg of native salmon sperm DNA per ml, 5% glycerol]. Due to the insolubility of the renatured His_{10}-OxyR, the amount of OxyR in the standard reaction mixture is only an approximation and probably represents an overestimate. After incubation for 10 min at room temperature, protein-DNA complexes were separated from the unbound probe on 4% native polyacrylamide gels in 6.7 mM Tris-HCl (pH 7.9)–3.3 mM sodium acetate–1 mM EDTA with buffer recirculation. The gels were dried and analyzed by autoradiography and densitometry where indicated.

Transcriptional fusion analyses using *xylE* as a reporter gene. Promoter activity was monitored by measuring catechol 2,3-dioxygenase (CDO) activity in *M. smegmatis* harboring *ahpC-xylE* transcriptional fusion constructs in accordance with previously described procedures (9). One unit of CDO is defined as the amount of enzyme oxidizing 1 μmol of catechol per min at 24°C.

Nucleotide sequence accession number. The DNA sequence of the *M. intracellulare oxyR-ahpC* intergenic region, obtained by using the previously described primers (11) and amplification of *M. intracellulare* genomic sequences by PCR, has been deposited in GenBank under accession number U71061.

RESULTS

Mapping of the *M. leprae oxyR* and *ahpC* mRNA 5′ ends. Since *oxyR* in *M. tuberculosis* contains multiple lesions, it is not possible to study regulatory relationships in this organism. However, a complete *oxyR* gene has been identified in *M. leprae* (2, 11). In our previous studies, we have analyzed the genomic clones of *oxyR* and *ahpC* from *M. leprae* and studied their effects on *M. tuberculosis* sensitivity to INH (11). Based on the rationale that understanding *M. leprae oxyR* and *ahpC* expression may also illuminate ancestral relationships preceding modern *M. tuberculosis*, here we initiated transcriptional analyses of the *M. leprae* genes. Since *M. leprae* cannot be cultivated in vitro, it was necessary to study expression of *oxyR* and *ahpC* in a heterologous host. We initially examined transcription of plasmid-borne *M. leprae oxyR* and *ahpC* in *M. smegmatis*, an organism frequently employed as a surrogate host in studies of gene expression in mycobacteria (20). *M. smegmatis* mc^{2}155 harboring plasmid pDML2 with a 2-kb insert containing the complete *M. leprae ahpC* and *oxyR* genes and the intergenic region carrying the putative *oxyR* and *ahpC* promoters was used to isolate RNA. The transcripts initiating within the *oxyR-ahpC* intergenic region were identified by S1 nuclease protection analysis (Fig. 2). The results of these experiments were consistent with the divergent transcription of *ahpC* and *oxyR* and indicated the presence of two mRNA 5′

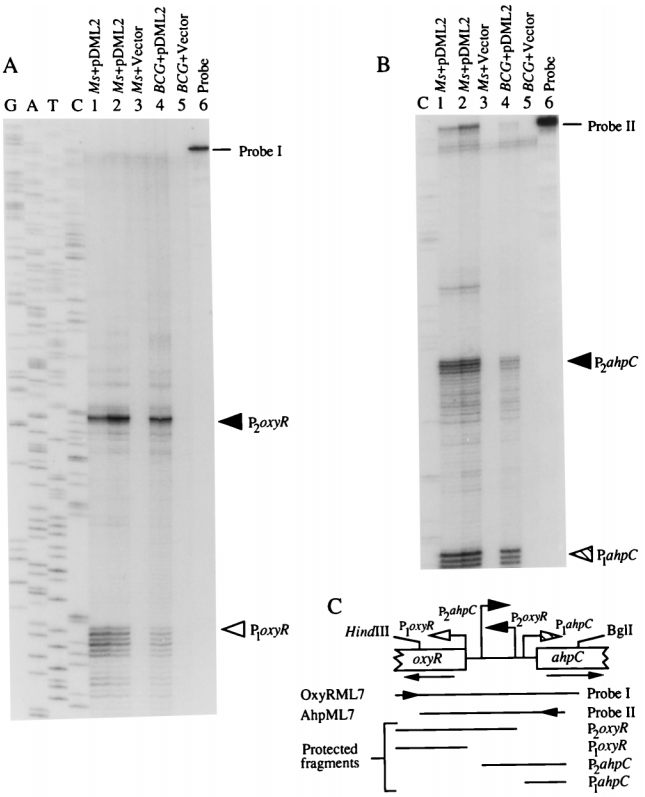

FIG. 2. Mapping of *M. leprae oxyR* and *ahpC* mRNA 5′ ends. S1 nuclease mapping of the 5′ mRNA ends was carried out, as described in Materials and Methods, by using RNAs from two hosts harboring plasmid-borne *oxyR-ahpC*: fast-growing *M. smegmatis* and slow-growing *M. bovis* BCG. Reaction products were analyzed on standard sequencing gels alongside the sequencing ladder generated by the same primer and template used to produce the probe (lane G, A, T, or C) and the undigested probe (lane 6 in both panels). (A) S1 nuclease protection analysis of *M. leprae oxyR* mRNA 5′ ends in *M. smegmatis* (*Ms*, lanes 1 to 3) and *M. bovis* BCG (lanes 4 and 5). Lanes: 1 and 2, 50 μg of RNA from *M. smegmatis* harboring plasmid pDML2 carrying a 2-kb insert with the complete *M. leprae oxyR* and *ahpC* genes; 3, 50 μg of RNA from *M. smegmatis* carrying the plasmid vector used to generate pDML2; 4, 50 μg of RNA from *M. bovis* BCG harboring plasmid pDML2; 5, 50 μg of RNA from *M. bovis* BCG harboring the plasmid vector. The S1 nuclease probe (see panel C and Materials and Methods) was generated by using pDML2 as the template and OxyRML7 as the primer with the 5′ end at position −234. The other end of the probe was defined by the *Bgl*I site at position +131 relative to the *ahpC* start codon. (B) S1 nuclease protection analysis of *M. leprae ahpC* mRNA 5′ ends in *M. smegmatis* (lanes 1 to 3) and *M. bovis* BCG (lanes 4 and 5). Quantities and RNA sources were identical to those in panel A. The S1 nuclease probe was generated by using primer AhpML7 (5′ end at position +76) and the same template as in panel A. The 3′ end of the probe was defined by the *Hin*dIII site (at position −198 relative to the *ahpC* start codon). (C) Schematic representation of the probes and protected fragments relative to the *M. leprae oxyR-ahpC* intergenic region.

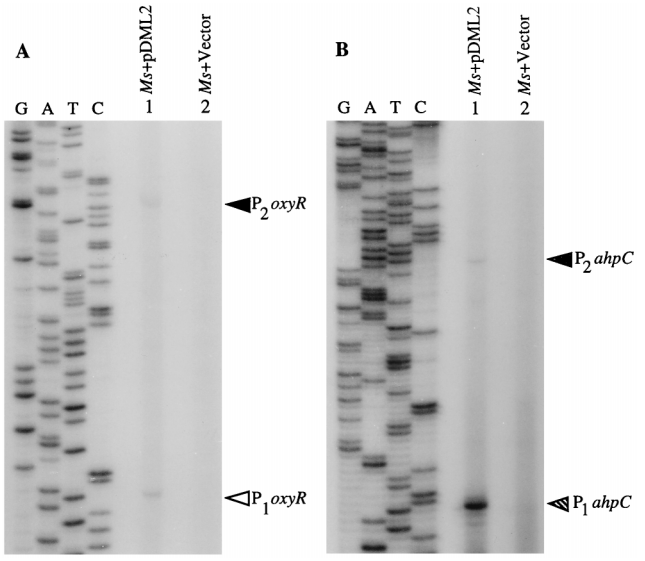

FIG. 3. Primer extension mapping of *M. leprae oxyR* and *ahpC* mRNA 5′ ends. Reverse transcription with end-labeled primers and total RNA was carried out as described in Materials and Methods. The products were analyzed on sequencing gels along with sequencing ladders (lanes G, A, T, and C) generated by using the same primers. (A) Primer extension of *oxyR* mRNA. (B) Primer extension of *ahpC* mRNA. Designations and patterns are the same as those in Fig. 2.

ends for both *oxyR* (Fig. 2A) and *ahpC* (Fig. 2B). To rule out the possibility that the presence of multiple mRNA start sites was due to expression in a fast-growing mycobacterium, we also introduced pDML2 into the slow-growing organism *M. bovis* BCG. When RNA was isolated from this host harboring the plasmid-borne *M. leprae ahpC* and *oxyR* genes, the same mRNA 5′ ends for each gene were detected (Fig. 2A and B, lanes 4). The mRNA 5′ ends were identical in both hosts and were specific for the pDML2 insert since the corresponding bands were absent in control samples with RNAs from *M. smegmatis* and *M. bovis* harboring the plasmid vector used to construct pDML2 (Fig. 2A and B, lanes 3). The locations of the mRNA 5′ ends were additionally confirmed by primer extension (reverse transcription) using RNA from *M. smegmatis* harboring pDML2 (Fig. 3). These experiments were consistent with the presence of tandemly organized transcriptional initiation sites for each gene, which were termed P_1*oxyR*, P_2*oxyR*, P_1*ahpC*, and P_2*ahpC*. While the majority of the transcripts in the *oxyR-ahpC* region are divergent relative to each other, typical of the LysR-type regulators and their linked subordinate genes, the P_2*ahpC* and P_2*oxyR* transcripts showed an overlap of 28 nucleotides. This peculiar arrangement resulted in a significant complementarity region at the 5′ ends of the P_2*ahpC* and P_2*oxyR* transcripts. Surprisingly, P_1*oxyR* coincided with the initiation codon of the *oxyR* gene. This feature is less commonly encountered in bacteria, with the notable exception of streptomycetes (44), a bacterial group considered to be closely related to mycobacteria.

Overproduction and purification of *M. leprae* OxyR. To determine whether *M. leprae* OxyR is a DNA binding protein and to investigate its potential interactions with the *oxyR-ahpC* intergenic region, we overproduced and purified OxyR. The coding region of *M. leprae oxyR* was cloned behind the T7 promoter in frame with the vector sequences encoding an N-terminal His_{10} tag to facilitate subsequent protein purification. When *E. coli* cells harboring the resulting *oxyR* overexpression construct pDML1 were exposed to IPTG to induce T7 promoter transcription, production of a novel 30-kDa polypeptide was observed (Fig. 4, lane 2). The apparent molecular mass of the overproduced polypeptide was 30 kDa, in keeping with the molecular mass expected for a His_{10}-OxyR hybrid. The majority of the 30-kDa polypeptide was found in insoluble pellets (Fig. 4, lanes 3 to 5), providing a significant purification step after differential centrifugation (Fig. 4, lane 5). The protein could be solubilized in urea and, as expected for a His_{10}-tagged product, displayed affinity for Ni^{2+}-NTA resin, which permitted its further enrichment (Fig. 4, lane 6). The purified polypeptide was transferred to an Immobilon-P membrane and subjected to digestion with cyanogen bromide and amino acid sequencing. For unknown reasons, this procedure did not yield an interpretable sequence. In an alternative approach, the protein was subjected to digestion in 80% formic acid for 3 days at 37°C, a procedure that hydrolyzes peptide bonds between consecutive Asp and Pro residues. The sequencing of the products of formic acid digestion yielded the sequence PLRXGMXLG LIP (X, uncertain residues), compatible with the predicted *M. leprae* OxyR sequence following the Asp residue at position 94. This analysis confirmed the identity of the purified protein as *M. leprae* OxyR. The purity of OxyR was >80% as judged by densitometry of Coomassie blue-stained gels (Fig. 4, lane 6).

Interactions of OxyR with the *oxyR-ahpC* intergenic region of *M. leprae* and *M. tuberculosis*. To test whether *M. leprae* OxyR functions as a DNA binding protein and whether it can form specific complexes with the region containing the mapped *oxyR* and *ahpC* promoters, we performed the following experiments. Radiolabeled DNA fragments containing the complete *oxyR-ahpC* intergenic regions from *M. leprae* (from −234 to +76 relative to the start codon of the *M. leprae ahpC* gene) and *M. tuberculosis* (from −146 to +104 relative to the start codon of the *M. tuberculosis ahpC* gene) were incubated with purified *M. leprae* OxyR, and formation of protein-DNA complexes was monitored on native polyacrylamide gels. The results of gel mobility shift studies are illustrated in Fig. 5. The *M. leprae* fragment displayed a single band of OxyR binding (Fig. 5A). This complex was sequence specific since experiments with specific competitor DNA (unlabeled DNA fragment identical

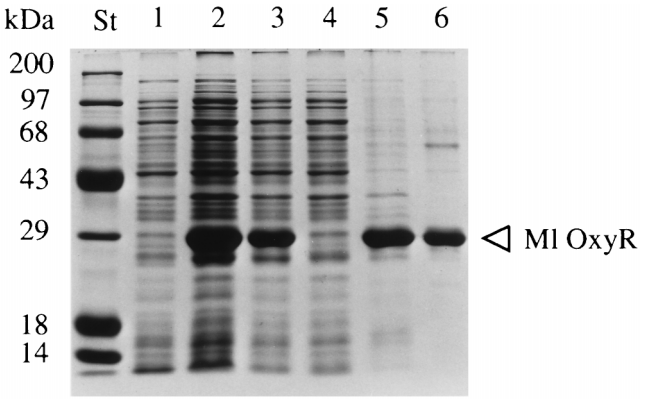

FIG. 4. Overproduction and purification of *M. leprae* OxyR. *E. coli* BL21 carrying *oxyR* expression plasmid pDML1 was grown in the absence or presence of 1 mM IPTG, and extracts were subjected to protein purification (see Materials and Methods). OxyR enrichment was monitored by sodium dodecyl sulfate-polyacrylamide gel electrophoresis and Coomassie blue staining. Lanes: 1, whole cell extract (no inducer); 2, whole cell extract after induction with 1 mM IPTG for 2 h; 3, French press lysate; 4, 10,000-rpm-centrifuged supernatant; 5, 10,000-rpm-centrifuged pellet; 6, His_{10}-OxyR after purification by affinity chromatography under denaturing conditions on Ni-NTA followed by renaturation (see Materials and Methods). Ml OxyR, *M. leprae* OxyR with N-terminal His_{10} tag.

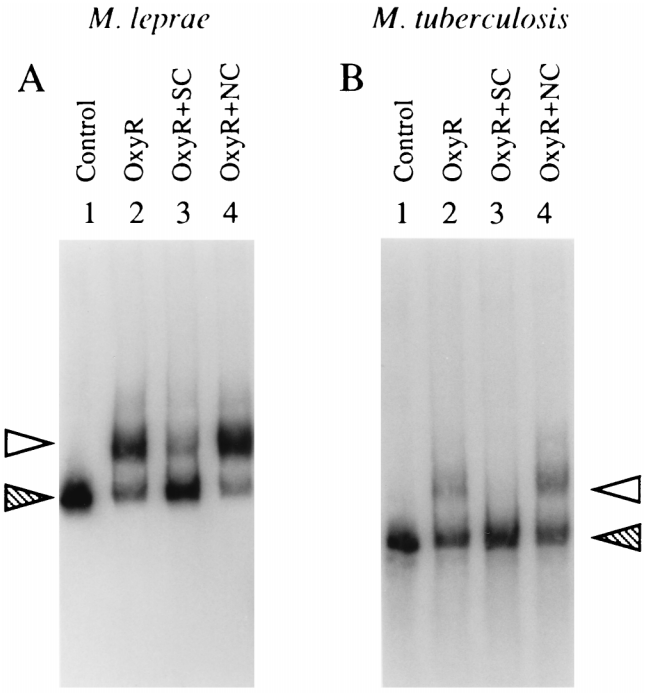

FIG. 5. DNA binding gel mobility shift assay and specificity of protein-DNA association of OxyR with *M. leprae* (A) and *M. tuberculosis* (B) *oxyR-ahpC*. OxyR was incubated with ^{32}P-labeled DNA fragments from *M. leprae* (310 bp) and *M. tuberculosis* (250 bp) containing the *oxyR-ahpC* intergenic region. Protein-DNA complexes (open triangles) were separated from unbound probes (hatched triangles) by electrophoresis on a 4% native polyacrylamide gel and analyzed by autoradiography. Lanes: 1, radiolabeled fragment alone; 2, 250 ng of His_{10}-OxyR; 3, 250 ng of His_{10}-OxyR and 1 μg of specific competitor (unlabeled DNA *M. leprae oxyR-ahpC* DNA fragment identical to the radiolabeled probe); 4, 250 ng of His_{10}-OxyR and 1 μg of unlabeled nonspecific competitor DNA (a 322-bp fragment spanning the region from +25 to +346 of the structural *M. leprae ahpC* gene).

to the probe used in the binding reaction) significantly reduced the amount of probe in the bound state (Fig. 5A, lane 3). In contrast, the same amount of nonspecific competitor DNA (a DNA fragment from +25 to +346 of the *M. leprae ahpC* structural gene) did not reduce formation of the OxyR-DNA complex (Fig. 5A, lane 4).

A similar set of experiments was carried out with the *oxyR-ahpC* intergenic region of *M. tuberculosis*, and the formation of a protein-DNA complex was observed (Fig. 5B, lane 2). The affinity of OxyR for the *M. tuberculosis* fragment was lower than that for the *M. leprae* fragment. This is evidenced by the finding that only 10% (determined by densitometry) of the *M. tuberculosis* probe was in the bound state (Fig. 5B, lane 2) under conditions which forced the majority of the *M. leprae* probe into the bound state (80%; Fig. 5A, lane 1). To demonstrate the specificity of interactions between OxyR and the *M. tuberculosis oxyR-ahpC* intergenic region, experiments with specific and nonspecific competitors were also carried out. These analyses indicated that the *M. leprae* fragment with the OxyR binding site, used as a specific competitor in Fig. 5A, effectively competed with the *M. tuberculosis* binding site (Fig. 5B, lane 3) while the nonspecific competitor DNA did not have a significant effect (Fig. 5B, lane 4). From these experiments, it is possible to conclude that both *M. leprae* and *M. tuberculosis* have a specific binding site for OxyR within the fragment carrying the *oxyR-ahpC* intergenic region and that the affinity for OxyR was higher in the case of *M. leprae*. The ability of the *M. leprae* fragment to compete for OxyR with the *M. tuberculosis* binding site suggested that the corresponding binding sites could be similar in nature but also indicated that there were likely differences within the putative recognition sequences.

Mapping of the OxyR binding site within the *M. leprae oxyR-ahpC* intergenic region. To delimit the OxyR binding site within the 310-bp DNA fragment containing the intergenic *oxyR-ahpC* region of *M. leprae*, two sequential series of overlapping probes with incremental removal of sequences from either end of the *ahpC-oxyR* region were generated by PCR (Fig. 1B details the endpoints of the fragments). Individual probes were radiolabeled and used in the OxyR binding assay. The series of fragments with the common end at +76 (relative to the *ahpC* initiation codon) and with the variable end ranging from −234 to −124 (Fig. 6A, lanes 1 to 4) showed OxyR binding similar to that of the full-size fragment used in Fig. 6A. However, when the variable end within this series of fragments changed from −124 (Fig. 6, lane 4) to −112 (Fig. 6, lane 5) or past that point (Fig. 6, lanes 6 and 7), the ability to bind OxyR was completely abrogated. A complementary set of experiments was carried out to delimit the other end of the OxyR binding site by using a series of fragments with the fixed end at −234 relative to the *ahpC* start codon and with the other end located between positions +76 and −115. When this set of probes was examined (Fig. 6A, lane 8, and Fig. 6B), it was found that the binding ability was lost only when deletions encroached on the region past position −95 (Fig. 6B, lanes 3 and 4). Thus, the endpoints of the fragments that permitted association with OxyR defined the region between −124 and −95 as the binding site for *M. leprae* OxyR. This was somewhat unexpected since this placed the OxyR binding site in a region spanning the initiation codon of *oxyR*. Nevertheless, this observation was consistent with the finding that the 5′ end of the P_1*oxyR* transcript also coincided with the first base of the coding region of *oxyR* (Fig. 1). This was in keeping with the usual autoregulatory overlap between the recognition se-

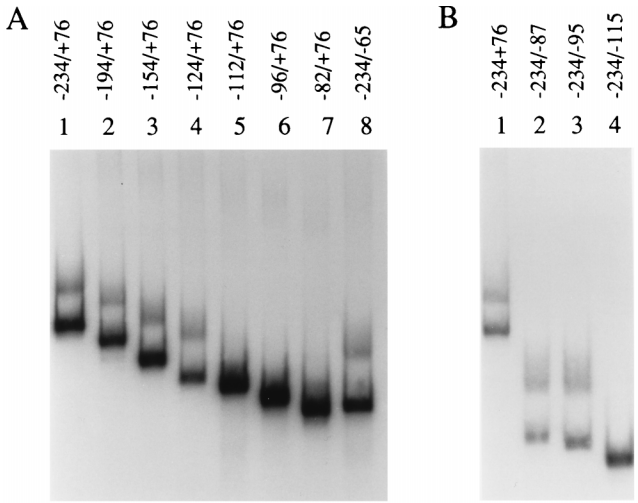

FIG. 6. Mapping of the OxyR binding site within the *M. leprae oxyR-ahpC* region by using a sequential series of overlapping DNA fragments generated by PCR. His_{10}-OxyR was incubated with radiolabeled DNA fragments (see Materials and Methods). Protein-DNA complexes were separated on 4% native polyacrylamide gels and analyzed by autoradiography. The reaction mixture in each lane contained the same amount of OxyR. Numbers above the lanes denote the 5′ ends of the primer pairs that were used to generate DNA probes by PCR (see Fig. 1A). (A) Mapping of the distal end of the OxyR binding site (lanes 1 to 7). (B) Lanes 1 to 4 (also, panel A, lane 8), mapping of the proximal end of the OxyR binding site.

quences for the gene products from the *lysR* superfamily of regulators and their own mRNA start sites (36). Furthermore, the mapped OxyR binding site was located at a position relative to *ahpC* typical of that of the LysR type of transcriptional factors in relation to the genes which they positively regulate. Next, we tested *ahpC* expression by using an *M. leprae ahpC-xylE* transcriptional fusion in *M. smegmatis* in the presence or absence of *M. leprae oxyR*. In these experiments, a statistically significant decrease in the baseline transcription of *ahpC* was observed when *oxyR* was absent: *M. smegmatis* harboring pDMLAX (*ahpC-xylE*) had a CDO (*xylE* gene product) activity of 4.6 ± 0.35 U/mg of protein, while *M. smegmatis* harboring pDMLAX/O ($oxyR^+$ *ahpC-xylE*) had a CDO activity of 7.5 ± 0.3 U/mg of protein ($P = 1.5 \times 10^{-4}$; [*t* test]).

Mycobacterial OxyR recognition sequence. LysR-type transcriptional regulators bind to a recognition sequence containing the characteristic T-N_{11}-A motif (17, 36). This motif is usually embedded within a longer palindromic sequence. *E. coli* OxyR has been recently reported to bind a duplication of the motif ATAGnTnnnAnCTAT (46). In this context, the region critical for the binding of *M. leprae* OxyR (Fig. 1, underlined sequence) was inspected for the presence of potential LysR-like motifs or sequences showing similarities to the *E. coli* OxyR recognition site. A sequence showing twofold dyad symmetry, CTTA**T**CactcataccG**A**TAAG (capital letters, palindromic sequence; lowercase letters, no symmetry; bold underlined nucleotides, T and A residues conforming with the core motif T-N_{11}-A), was observed centered within the 30-bp region critical for OxyR binding (Fig. 1). This putative OxyR recognition sequence was located 65 bp upstream of the P_1*ahpC* start site, typical of the LysR-type transcriptional regulators, which bind the primary recognition sequence positioned, on average, 65 bp upstream of the mRNA start site (36). Next, we wanted to compare this sequence with those of the corresponding regions from other mycobacteria. The sequence of this region has been reported for *M. avium* (48) and showed strong similarities to the proposed recognition sequence, but the distance between the T and A corresponding to the proposed T-N_{11}-A core was only 10 bp. However, examination of a more recent report (38) indicated a conflict in this region with the previously published sequence (48). To clarify these discrepancies, we reexamined this region and also determined the sequence of the intergenic *oxyR-ahpC* region from *M. intracellulare*. These analyses showed that in both *M. intracellulare* and *M. avium*, which had identical sequences in this entire region, there were 11 nucleotides in the critical region (Fig. 7; only the *M. avium* sequence is displayed to avoid redundancies). This sequence in *M. intracellulare* and *M. avium* showed a conservation of the palindromic structure extending further towards the center of the dyad symmetry (Fig. 7). Based on the available sequences, it was possible to derive a mycobacterial OxyR consensus recognition sequence (Fig. 7) which showed only limited similarity to the *E. coli* OxyR recognition sequence (46). However, it contained the T-N_{11}-A motif considered to represent the signature core of all LysR-type recognition sequences. In keeping with the differences relative to *E. coli* concerning the recognition sequences (Fig. 7) and an apparently smaller region involved in interactions with mycobacterial OxyR (46), we found that the *M. leprae oxyR-ahpC* DNA fragment did not bind *E. coli* OxyR (data not shown). Interestingly, while the overall dyadic symmetry was preserved within the corresponding region of *M. tuberculosis*, extending even further towards the center of the palindrome, the left half-site in this organism has deviated from the T-N_{11}-A rule (17, 36) by having a substitution in place of the T residue. Considering the otherwise exceptionally high sequence conservation in different mycobacteria (including *M. tuberculosis*) within the 30-bp segment binding OxyR, this anomaly could account for the observed lower apparent affinity of OxyR for the *M. tuberculosis oxyR-ahpC* region (Fig. 5B).

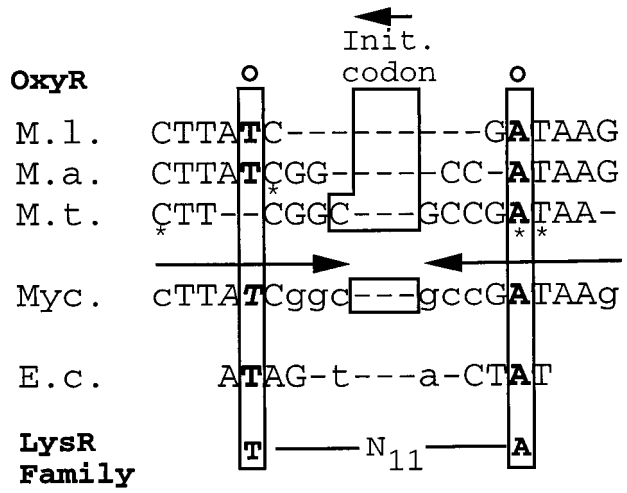

FIG. 7. Compilation of the putative mycobacterial OxyR recognition sequences. Shown are sequences located at equivalent positions within the *oxyR-ahpC* intergenic region of *M. leprae* (M.l.), *M. avium* (M.a.), and *M. tuberculosis* (M.t.). The *M. avium* sequence, about which there have been conflicting reports on the region of interest (38, 48), was verified and was identical to that determined for *M. intracellulare*. Myc., mycobacterial OxyR consensus recognition sequence derived in this work. E.c., *E. coli* OxyR consensus recognition sequence (46). The actual bases are displayed only (with the exception of nucleotides marked with asterisks) if they form a sequence with dyad symmetry (convergent arrows). Unshaded boxed nucleotides (and circles), the core sequence T-N_{11}-A typically embedded within the palindromic recognition sequence of the LysR-type transcriptional regulators (46). Shaded boxed area, location of the *oxyR* initiation codon (antisense strand, as indicated by the overhead arrow). The extended shaded box in the case of *M. tuberculosis* reflects the inversion of two nucleotides destroying the start codon of *oxyR* in this organism (11). Dashes, residues not conforming with the consensus sequence or positions of lesser or no conservation. Lowercase letters, positions with relaxed conservation. Asterisks below nucleotides, conserved residues conforming with the consensus sequence but lacking the symmetrical counterpart. Italicized nucleotides, bases corresponding to the positions altered in *M. tuberculosis* believed to cause the reduced affinity for OxyR.

DISCUSSION

In this work, we have purified *M. leprae* OxyR, demonstrated that it is a DNA binding protein, and delimited its binding site within the *oxyR-ahpC* intergenic region of *M. leprae* and *M. tuberculosis*. These findings are consistent with the proposals, founded on sequence similarities (11, 13, 38), that mycobacterial OxyR may have a regulatory function. In a complementary set of experiments, we have mapped the 5′ ends of *M. leprae oxyR* and *ahpC* transcripts expressed in two mycobacterial hosts. The position of *M. leprae* P_1*ahpC* matches, within one nucleotide, the location of the previously mapped *ahpC* mRNA start site of *M. bovis* BCG (50), further supporting the conclusion that this mRNA 5′ end is the major transcriptional start site for *ahpC*. It is nevertheless not possible, based on the available experimental evidence, to rule out the possibility that the shorter P_1 transcripts represent processing products of the longer P_2 transcripts. However, we do not favor this possibility for the following reasons. (i) In the case of P_1*oxyR*, this mRNA 5′ end overlaps the center of the OxyR recognition sequence, characteristic of the autoregulatory relationships within the LysR superfamily factors which bind to the transcription initiation site of their own genes. (ii) In the case of P_1*ahpC*, this

mRNA start site is positioned at −65 relative to the recognition site of OxyR, a distance typical of LysR-type regulators (36). (iii) The P_1*ahpC* transcript is the only strong signal that has been detected for chromosomal *M. bovis ahpC* (50).

The presence of multiple mRNA 5′ ends in the *oxyR-ahpC* intergenic region is suggestive of complex regulation of *ahpC* and *oxyR* expression. The role of the arrangement involving a pair of divergently oriented mRNA molecules (P_2*ahpC* and P_2*oxyR*) with a region of complementarity at their 5′ ends is not known. In other systems, short regions of complementarity in different RNA molecules have been implicated in transcriptional (33) or posttranscriptional control (31, 40). Although this type of regulation is relatively uncommon, it is interesting that of the few known examples, two belong to oxidative response systems: (i) *micF* RNA, which affects translation of *ompF* mRNA based on its complementarity to the 5′ end of the *ompF* transcript (31), is part of the oxidative stress response in *E. coli* (6), and (ii) the product of *oxyS*, a gene divergently transcribed from and controlled by *oxyR* in *E. coli*, is a small, untranslated RNA proposed to play a regulatory role (46).

It is of further interest that although P_1*oxyR* coincides with the initiation codon of *oxyR*, this somewhat unexpected finding is not without precedents. For example, there are at least 11 genes in actinomycetes, with the majority of characterized cases being in members of the genus *Streptomyces* closely related to mycobacteria, with transcriptional start sites coinciding with the start codon of the corresponding gene (44). This phenomenon is not limited to streptomycetes and includes examples in other organisms, such as the *prm* promoter of the λ *c*I gene (35) and the *polA* promoter in *Streptococcus pneumoniae* (28). One suggestion that has been offered to explain the rather common occurrence of such a gene structure in streptomycetes (44) is the possibility that ribosomes in these organisms do not require extended complementarity of the mRNA template and the 3′ end of 16S rRNA. The recent efficient expression in mycobacteria (12, 23) of a eucaryotic cDNA encoding green fluorescent protein, even when devoid of obvious Shine-Dalgarno sequences (12), seems to support such notions. An alternative view that OxyR, as a regulatory factor, may need to be produced in only small amounts, which could be achieved by inefficient translation, appears less likely since transcriptional and translational start sites also coincide in some of the highly expressed genes (e.g., *aph* and *rph*) in streptomycetes (44).

The proposed recognition sequence for mycobacterial OxyR (cTTATCggc-N_3-gccGATAAg) is well conserved in the majority of characterized mycobacteria and in several additional mycobacterial species for which characterization of the *oxyR-ahpC* region is under way (34). Most LysR-type transcriptional regulators bind to a primary recognition sequence which is almost invariably a palindrome containing the core T-N_{11}-A motif embedded within a longer dyadic sequence (17, 36). This also appears to be the case with *M. leprae* OxyR and its recognition sequence (Fig. 7). It is worth noting that *M. tuberculosis* has retained several aspects of the dyad symmetry but also displays a marked departure from the core motif within its left half site, where the triplet ATC has changed into ggC (lowercase letters, variance with the consensus sequence), destroying the core T-N_{11}-A motif (Fig. 7). This divergence, which stands out against the background of other highly conserved sequences in this region, may explain the observed lower affinity of purified OxyR for the *M. tuberculosis oxyR-ahpC* fragment (Fig. 4B). In the context of the loss of *oxyR* function in *M. tuberculosis*, the departure from the consensus OxyR recognition sequence may be added to the list of lesions affecting the OxyR system in *M. tuberculosis* (11).

In contrast to the recognition sequence in enteric bacteria, which until very recently (46) could not be easily deduced due to its poor conservation, the mycobacterial OxyR recognition sequence appears to be well preserved, at least in the *oxyR-ahpC* promoter region. This difference may reflect the nature of *E. coli* OxyR, which is a tetramer and binds to sequences that represent a duplication of the basic palindrome (46). *E. coli* OxyR binding is distributed over a longer region that provides specific contacts, thus allowing significant deviations from the consensus ATAG-T- - - -A-CTAT within individual sites. By comparison, the mycobacterial OxyR binding site corresponds to a half of the *E. coli* OxyR binding site. However, its almost perfect palindromic sequence and apparent preservation in different species may provide sufficient specificity for mycobacterial OxyR binding in lieu of a longer recognition sequence. While the multimerization state of *M. leprae* OxyR is not known, it is likely that OxyR binds the proposed OxyR recognition sequence as a dimer. Although this does not absolutely preclude higher-order interactions, we have observed only one specific protein-DNA complex in our experiments. Furthermore, deletion of sequences beyond the minimal region necessary for *M. leprae* OxyR binding did not seem to alter the affinity of OxyR for the *oxyR-ahpC* promoter region. For example, the series of fragments with one end at −234 and the other end located between +76 and −95 (Fig. 6A, lane 8, and Fig. 6B, lanes 1 to 3) displayed similar apparent affinities for OxyR. Moreover, there was no recognizable mycobacterial OxyR consensus sequence in the region between the end of the identified OxyR binding site and the P_1*ahpC* mRNA start.

In addition to the well-defined primary recognition sequence, LysR-type regulators in many instances interact with a region closer to the −35 promoter region which does not necessarily have to resemble the consensus binding site. The occupancy of this second site, sometimes referred to as the activation site (36), often depends on a coinducer or an external signal which induces protein-protein interactions, albeit with the notable exception of some (but not all) tetrameric LysR-like proteins (5, 25, 36, 46). Such processes are considered to play a role in promoter activation in response to external stimuli (36). In our attempts, we have not been able to detect, within the limitations of the gel mobility shift DNA binding assay, occupancy of any potential sites downstream of the primary recognition sequence. When *E. coli* OxyR is reduced in the presence of 100 mM DTT, depending upon the promoter, this either diminishes OxyR binding or repositions the contacts of the OxyR tetramer (43, 46). In preliminary experiments, treatments with 100 mM DTT did not affect the affinity of *M. leprae* OxyR for its *oxyR-ahpC* binding site, although mycobacterial OxyR is believed (11) to contain the highly conserved redox-sensitive center corresponding to Cys-199 in *E. coli* OxyR (26). Since the OxyR used in our studies has been subjected to a denaturation-renaturation cycle in vitro, perhaps the formation of higher multimeric structures is not possible or is not efficient in such preparations, thus precluding the detection of additional contacts that may occur with the native protein in vivo. Further analyses are needed to investigate these possibilities and how OxyR participates in the regulation of promoters identified in the *oxyR-ahpC* region.

In our analyses using an *ahpC-xylE* transcriptional fusion in *M. smegmatis*, we detected a limited role for OxyR in the baseline level of *ahpC* transcription. However, we did not observe induction of *ahpC* expression in response to challenges with 125 μM H_2O_2 or cumene hydroperoxide (data not shown), although this peroxide concentration is known to induce a vigorous response in *M. smegmatis* (13). It is possible that the use of a heterologous host and plasmid-borne fusions

precluded efficient signal recognition or that some other aspects of *M. leprae* OxyR function were affected. Studies have been initiated to examine mycobacterial OxyR function and *ahpC* induction in response to oxidative stress in the native environment by using other mycobacterial species (e.g., *M. marinum* and *M. xenopi*) that appear to have this system intact. Initial analyses indicate that *ahpC* can be induced by H_2O_2 treatment in both *M. marinum* and *M. xenopi*, whose *oxyR-ahpC* organization is similar to that of *M. leprae* and *M. tuberculosis* (34).

The studies aimed at understanding how OxyR functions in mycobacteria and how *oxyR* deficiency in *M. tuberculosis* affects oxidative stress response systems in this organism have fundamental biological value but also possess practical significance in the context of the mode of action of the potent antituberculosis agent INH. In addition to the pathways of INH action which include InhA and mycolic acids, it is also known that this drug, in reaction with KatG in the presence of *M. tuberculosis* extracts (39) or during auto-oxidation catalyzed by transition metals (24, 49), generates reactive oxygen intermediates that may have a more general damaging effect on mycobacterial cells. In the context of these models of INH action, alkyl hydroperoxide reductase, and perhaps other putative members of the oxidative stress response in mycobacteria, may reduce peroxide products or protect from oxidation particularly sensitive targets such as nucleic and unsaturated fatty acids. Alternatively or in addition, AhpC may directly detoxify the activated INH. Consequently, any defect in activity of the corresponding genes (e.g., diminished or unresponsive expression due to the loss of *oxyR* function) could contribute to the overall sensitivity of *M. tuberculosis* to INH. In a recent demonstration of the critical role of such phenomena for mycobacterial susceptibility to INH, insertional inactivation of *ahpC* in *M. smegmatis* caused increased sensitivity to INH in this organism (50). Nevertheless, it is likely that factors in addition to *ahpC* levels contribute to the exquisite susceptibility of *M. tuberculosis* to INH. The experiments described in this work, the availability of purified OxyR, and the definition of the OxyR recognition sequence should facilitate future studies addressing the natural sensitivity of the tubercle bacillus to INH and foster intensified explorations of the oxidative stress response systems in *M. tuberculosis* and other mycobacteria.

ACKNOWLEDGMENTS

We thank G. Storz for the gift of *E. coli* OxyR and E. Págan-Ramos for comments.

This work was supported by grant AI25217 from the National Institute of Allergy and Infectious Diseases.

REFERENCES

1. **Ausubel, F. M., R. Brent, R. E. Kingston, D. D. Moore, J. G. Seidman, J. A. Smith, and K. Struhl.** 1989. Current protocols in molecular biology. John Wiley & Sons, Inc., New York, N.Y.
2. **Bergh, S., and S. T. Cole.** 1994. MycDB: an integrated mycobacterial database. Mol. Microbiol. **12:**534–574.
3. **Burke, J. F.** 1984. High-sensitivity S1 mapping with single-stranded [^{32}P] DNA probes synthesized from bacteriophage M13mp templates. Gene **30:** 63–68.
4. **Chae, H. Z., K. Robinson, L. B. Poole, G. Church, G. Storz, and S. G. Rhee.** 1994. Cloning and sequencing of thiol-specific antioxidant from mammalian brain: alkyl hydroperoxide reductase and thiol-specific antioxidant define a large family of antioxidant enzymes. Proc. Natl. Acad. Sci. USA **91:**7017–7021.
5. **Chang, M., and I. P. Crawford.** 1991. In vitro determination of the effect of indoleglycerol phosphate on the interaction of purified TrpI protein with its DNA-binding sites. J. Bacteriol. **173:**1590–1597.
6. **Chou, J. H., J. T. Greenberg, and B. Demple.** 1993. Posttranscriptional repression of *Escherichia coli* OmpF protein in response to redox stress: positive control of the *micF* antisense RNA by the *soxRS* locus. J. Bacteriol. **175:**1026–1031.
7. **Christman, M. F., R. W. Morgan, F. S. Jacobson, and B. N. Ames.** 1985. Positive control of a regulon for defences against oxidative stress and some heat-shock proteins in *Salmonella typhimurium*. Cell **41:**753–762.
8. **Clemens, D. L., and M. A. Horwitz.** 1995. Characterization of the *Mycobacterium tuberculosis* phagosome and evidence that phagosomal maturation is inhibited. J. Exp. Med. **181:**257–270.
9. **Curcic, R., S. Dhandayuthapani, and V. Deretic.** 1994. Gene expression in mycobacteria: transcriptional fusions based on *xylE* and analysis of the promoter region of the response regulator *mtrA* from *Mycobacterium tuberculosis*. Mol. Microbiol. **13:**1057–1064.
10. **Deretic, V., E. Pagan-Ramos, Y. Zhang, S. Dhandayuthapani, and L. E. Via.** 1996. The exquisite sensitivity of *Mycobacterium tuberculosis* to the front-line antituberculosis drug isoniazid. Nat. Biotechnol. **14:**1557–1561.
11. **Deretic, V., W. Philipp, S. Dhandayuthapani, M. H. Mudd, R. Curcic, T. Garbe, B. Heym, L. E. Via, and S. T. Cole.** 1995. *Mycobacterium tuberculosis* is a natural mutant with an inactivated oxidative-stress regulatory gene: implications for sensitivity to isoniazid. Mol. Microbiol. **17:**889–900.
12. **Dhandayuthapani, S., L. E. Via, C. A. Thomas, P. M. Horowitz, D. Deretic, and V. Deretic.** 1995. Green fluorescent protein as a marker for gene expression and cell biology of mycobacterial interactions with macrophages. Mol. Microbiol. **17:**901–912.
13. **Dhandayuthapani, S., Y. Zhang, M. H. Mudd, and V. Deretic.** 1996. Oxidative stress response and its role in sensitivity to isoniazid in mycobacteria: characterization and inducibility of *ahpC* by peroxides in *Mycobacterium smegmatis* and lack of expression in *M. aurum* and *M. tuberculosis*. J. Bacteriol. **178:**3641–3649.
14. **Fenton, M. J., and M. W. Vermeulen.** 1996. Immunopathology of tuberculosis: roles of macrophages and monocytes. Infect. Immun. **64:**683–690.
15. **Garbe, T., J. Barathi, S. Barninin, Y. Zhang, C. Abou-Zeid, R. Tang, R. Mukherjee, and D. Young.** 1994. Transformation of a range of mycobacterial species using hygromycin resistance as a selectable marker. Microbiology **140:**133–138.
16. **Garbe, T. R., N. S. Hibler, and V. Deretic.** 1996. Response of *Mycobacterium tuberculosis* to reactive oxygen and nitrogen intermediates. Mol. Med. **2:**134–142.
17. **Goethals, K., M. VanMontagu, and M. Holsters.** 1992. Conserved motifs in a divergent *nod* box of *Azorhizobium caulinodans* ORS571 reveal a common structure in promoters regulated by LysR-type proteins. Proc. Natl. Acad. Sci. USA **89:**1646–1650.
18. **Henikoff, S., W. Haughn, J. M. Calvo, and J. C. Wallace.** 1989. A large family of bacterial activator proteins. Proc. Natl. Acad. Sci. USA **85:**6602–6606.
19. **Heym, B., P. M. Alzari, N. Honore, and S. T. Cole.** 1995. Missense mutations in the catalase-peroxidase gene, *katG*, are associated with isoniazid resistance in *Mycobacterium tuberculosis*. Mol. Microbiol. **15:**235–245.
20. **Jacobs, W. R., G. V. Kalpana, J. D. Cirrilo, L. Pascopella, S. B. Snapper, R. A. Udani, W. Jones, R. G. Barletta, and B. R. Bloom.** 1991. Genetic systems for mycobacteria. Methods Enzymol. **204:**537–555.
21. **Jacobson, F. S., R. W. Morgan, M. F. Christman, and B. N. Ames.** 1989. An alkyl hydroperoxide reductase from *Salmonella typhimurium* involved in the defense of DNA against oxidative damage. J. Biol. Chem. **264:**1488–1496.
22. **Kaufmann, S. H. E., and I. E. A. Flesch.** 1992. Life within phagocytic cells, p. 97–106. *In* C. E. Hormachie, C. W. Penn, and C. J. Smyth (ed.), Molecular biology of bacterial infection. Cambridge University Press, Cambridge, England.
23. **Kremer, L., A. Baulard, J. Estaquier, O. Poulain-Godefroy, and C. Locht.** 1995. Green fluorescent protein as a new expression marker in mycobacteria. Mol. Microbiol. **17:**913–922.
24. **Kruger-Thiemer, E.** 1958. Isonicotinic acid hypothesis of the antituberculous action of isoniazid. Am. Rev. Tuberc. **77:**364–367.
25. **Kullik, I., J. Stevens, M. B. Toledano, and G. Storz.** 1995. Mutational analysis of the redox-sensitive transcriptional regulator OxyR: regions important for DNA binding and multimerization. J. Bacteriol. **177:**1285–1291.
26. **Kullik, I., M. B. Toledano, L. A. Tartaglia, and G. Storz.** 1995. Mutational analysis of the redox-sensitive transcriptional regulator OxyR: regions important for oxidation and transcriptional activation. J. Bacteriol. **177:**1275–1284.
27. **Le Lirzin, M. J. N., J. N. Vivien, A. Lepeuple, R. Thibier, and C. Pretet.** 1971. Rapid microbiological estimation of serum isoniazid. Rev. Tuberc. Pneumol. **35:**350–356.
28. **Lopez, P., S. Martinez, A. DIaz, M. Espinoza, and S. A. Lacks.** 1989. Characterization of the *polA* gene of *Streptococcus pneumoniae* and comparison of the DNA polymerase I it encodes to homologous enzymes from *Escherichia coli* and phage T7. J. Biol. Chem. **264:**4255–4263.
29. **McDonough, K. A., and Y. Kress.** 1995. Cytotoxicity for lung epithelial cells is a virulence-associated phenotype of *Mycobacterium tuberculosis*. Infect. Immun. **63:**4802–4811.
30. **Middlebrook, G.** 1954. Isoniazid-resistance and catalase activity of tubercle bacilli. Am. Rev. Tuberc. **69:**471–472.
31. **Mizuno, T., K. Masashi, Y. Jo, and S. Mizushima.** 1984. A unique mechanism regulating gene expression: translational inhibition by a complementary RNA transcript (micRNA). Proc. Natl. Acad. Sci. USA **81:**1966–1970.
32. **Musser, J. M.** 1995. Antimicrobial agent resistance in mycobacteria: molec-

ular genetic insights. Clin. Microbiol. Rev. **8:**496–514.
33. **Okamoto, K., and M. Freundlich.** 1986. Mechanism for the autogenous control of the *crp* operon: transcriptional inhibition by a divergent RNA transcript. Proc. Natl. Acad. Sci. USA **83:**5000–5004.
34. **Pagan-Ramos, E., M. Mudd, and V. Deretic.** Unpublished results.
35. **Ptashne, M., K. Backman, M. Z. Humayun, A. Jeffrey, R. Maurer, B. Meyer, and R. T. Sauer.** 1976. Autoregulation and function of a repressor in bacteriophage lambda. Science **194:**156–161.
36. **Schell, M. A.** 1993. Molecular biology of the LysR family of transcriptional regulators. Annu. Rev. Microbiol. **47:**597–626.
37. **Sherman, D. R., K. Mdluli, M. J. Hickey, T. M. Arain, S. L. Morris, C. E. Barry, and C. K. Stover.** 1996. Compensatory *ahpC* gene expression in isoniazid-resistant *Mycobacterium tuberculosis*. Science **272:**1641–1643.
38. **Sherman, D. R., P. J. Sabo, M. J. Hickey, T. M. Arain, G. G. Mahairas, Y. Yuan, C. E. Barry, and C. K. Stover.** 1995. Disparate responses to oxidative stress in saprophytic and pathogenic mycobacteria. Proc. Natl. Acad. Sci. USA **92:**6625–6629.
39. **Shoeb, H. A., B. U. Bowman, A. C. Ottolenghi, and A. J. Merola.** 1985. Evidence for the generation of active oxygen by isoniazid treatment of extracts of *Mycobacterium tuberculosis* H37Ra. Antimicrob. Agents Chemother. **27:**404–407.
40. **Simons, R. W., and N. Kleckner.** 1988. Biological regulation by antisense RNA in prokaryotes. Annu. Rev. Genet. **22:**567–600.
41. **Snapper, S. B., R. E. Melton, S. Mustafa, T. Kieser, and W. R. Jacobs.** 1990. Isolation and characterization of efficient plasmid transformation mutants of *Mycobacterium smegmatis*. Mol. Microbiol. **4:**1911–1919.
42. **Sreevatsan, S., P. Escalante, X. Pan, D. A. Gillies, II, S. Siddiqui, C. N. Khalaf, B. N. Kreiswirth, P. Bifani, L. G. Adams, T. Ficht, V. S. Perumaalla, M. D. Cave, J. D. A. van Embden, and J. M. Musser.** 1996. Identification of a polymorphic nucleotide in *oxyR* specific for *Mycobacterium bovis*. J. Clin. Microbiol. **34:**2007–2010.
43. **Storz, G., L. A. Tartaglia, and B. N. Ames.** 1990. Transcriptional regulator of oxidative stress-inducible genes: direct activation by oxidation. Science **248:** 189–194.
44. **Strohl, W. R.** 1992. Compilation and analysis of DNA sequences associated with apparent streptomycete promoters. Nucleic Acids Res. **20:**961–974.
45. **Sturgill-Koszycki, S., P. H. Schlesinger, P. Chakraborty, P. L. Haddix, H. L. Collins, A. K. Fok, R. D. Allen, S. L. Gluck, J. Heuser, and D. G. Russell.** 1994. Lack of acidification in *Mycobacterium* phagosomes produced by exclusion of the vesicular proton-ATPase. Science **263:**678–681.
46. **Toledano, M. B., I. Kullik, F. Trinh, P. T. Baird, T. D. Schneider, and G. Storz.** 1994. Redox-dependent shift of OxyR-DNA contacts along an extended DNA-binding site: a mechanism for differential promoter selection. Cell **78:**897–909.
47. **Wilson, T. M., and D. M. Collins.** 1996. *ahpC*, a gene involved in isoniazid resistance of the *Mycobacterium tuberculosis* complex. Mol. Microbiol. **19:** 1025–1034.
48. **Yamaguchi, R., K. Matsuo, A. Yamazaki, M. Takahashi, Y. Fukusawa, M. Wada, and C. Abe.** 1992. Cloning and expression of the gene for the Avi-3 antigen of *Mycobacterium avium* and mapping of its epitopes. Infect. Immun. **60:**1210–1216.
49. **Youatt, J.** 1969. A review of the action of isoniazid. Am. Rev. Respir. Dis. **99:**729–749.
50. **Zhang, Y., S. Dhandayuthapani, and V. Deretic.** 1996. Molecular basis for the exquisite sensitivity of *Mycobacterium tuberculosis* to isoniazid. Proc. Natl. Acad. Sci. USA **93:**13212–13216.
51. **Zhang, Y., B. Heym, B. Allen, D. Young, and S. T. Cole.** 1992. The catalase-peroxidase gene and isoniazid resistance of *Mycobacterium tuberculosis*. Nature **358:**591–593.
52. **Zhang, Y., and D. B. Young.** 1993. Molecular mechanisms of isoniazid: a drug at the front line of tuberculosis control. Trends Microbiol. **1:**109–113.